ATMOSPHERIC SCIENCE LETTERS
Atmos. Sci. Let. **6**: 23–30 (2005)
Published online 22 February 2005 in Wiley InterScience (www.interscience.wiley.com). **DOI:** 10.1002/asl.86

Rainfall modeling for integrating radar information into hydrological model

Efrat Morin,[1]* David C. Goodrich,[2] Robert A. Maddox,[3] Xiaogang Gao,[4] Hoshin V. Gupta[5] and Soroosh Sorooshian[4]

[1]*Department of Geography, Hebrew University of Jerusalem, Jerusalem, Israel*
[2]*USDA-ARS, Southwest Watershed Research Center, Arizona, USA*
[3]*Department of Atmospheric Sciences, University of Arizona, Arizona, USA*
[4]*Department of Civil and Environmental Engineering, University of California, California, USA*
[5]*Department of Hydrology and Water Resources, University of Arizona, Arizona, USA*

**Correspondence to:*
Efrat Morin, Department of Geography, Hebrew University of Jerusalem, Jerusalem, 91905, Israel.
E-mail: msmorin@mscc.huji.ac.il

Received: 28 June 2004
Revised: 18 November 2004
Accepted: 18 November 2004

Abstract

A spatial rainfall model was applied to radar data of air mass thunderstorms to yield a rainstorm representation as a set of convective rain cells. The modeled rainfall was used as input into hydrological model, instead of the standard radar-grid data. This approach allows a comprehensive linkage between runoff responses and rainfall structures. Copyright © 2005 Royal Meteorological Society

Keywords: spatial patterns; rainfall; weather radar; conceptual modeling; thunderstorms; distributed hydrological models

1. Introduction

Complex interactions exist between the spatiotemporal structure of rain systems and watershed hydrological response. While this is a long-standing research issue in hydrology, a comprehensive study of these interactions requires detailed rainfall data in space and time that were effectively unavailable until recently.

For many years, rain gauge networks were the primary source of storm data. However, these networks are typically sparse and the recorded rainfall data do not adequately represent the spatial variability of the storm (e.g., Michaud and Sorooshian, 1994). In recent years, a new type of rainfall data, coming from weather radar systems, has become available. This new technology permits a detailed view of the rainstorm over the watershed with high spatial and temporal resolution. Access to reliable information on different storm characteristics, such as the location of the storm over the watershed and its structure and moving direction, presents a new stage in rainfall-runoff analysis.

It was hoped that the use of detailed radar rainfall information as input into hydrological models representing the watershed hydrological response would significantly improve understanding of rainfall-runoff processes and help in predicting their outcome. However, a review of studies using radar rainfall data in hydrological modeling (e.g. Collinge and Kirby, 1987; Julien *et al*., 1995) does not provide clear evidence for any such improvements (e.g., Carpenter *et al*., 2001). Among the difficulties reported were the inaccuracy of radar rainfall estimations (e.g., Krajewski and Smith, 2002) and runoff sensitivity to subpixel rainfall variability (e.g., Michaud and Sorooshian, 1994; Winchell *et al*., 1998; Ichikawa *et al*., 2002). Arguably, even though information about rainfall structures exists in radar rainfall data, it is but only implicitly represented. As a result, the major strength of this source of information is not fully exploited.

In the current study, we suggest explicitly representing the rainfall through application of a rainfall model. This approach will allow a direct linkage between rainfall structures and watershed hydrological response by means of hydrological modeling. The article focuses on modeling spatial structures of rainfall in air mass thunderstorm events. The rainfall model is applied to radar data and is evaluated using a dense gauge network. For a case study, the modeled rainfall is applied to a distributed hydrological model and the sensitivity of runoff response to rainfall pattern is examined.

2. Background

The study area is the 148 km^2 Walnut Gulch Experimental Watershed (WGEW; Goodrich *et al*., 1997) located in the semiarid climate regime of southeastern Arizona (Figure 1). The summer weather of this region is strongly affected by the North American monsoon (Douglas *et al*., 1993; Wallace *et al*., 1999), which results in frequent air mass thunderstorms that are highly convective, intense, localized and of short duration.

Thirteen convective storms from the 1999 and 2000 monsoon seasons were analyzed in the study (Table I). For one of the storms (August 11, 2000), a hydrological model was applied.

The watershed is equipped with a dense network of rainfall gauges (Figure 1) managed by the Agriculture

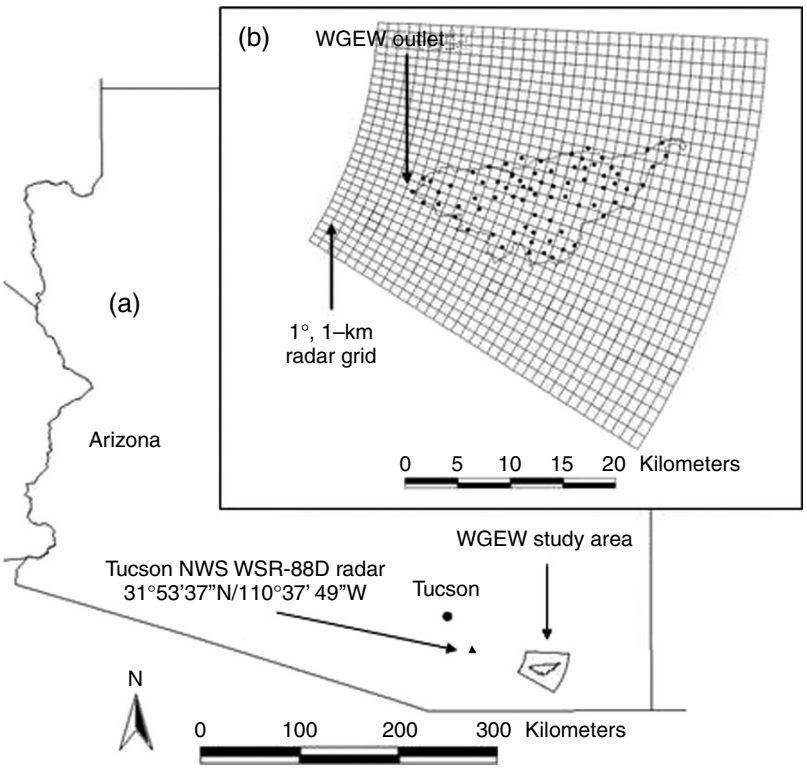

Figure 1. (a) Location map of the study area and the radar station. (b) The radar segment (azimuth: 93–122° and range: 42–78 km relative to the Tucson radar) encompassing the 148 km^2 WGEW study area and the 74 gauges in the watershed. Radar polar grid resolution is of 1° × 1 km

Table I. Storm characteristics

Storm	Study area	Local start time	Duration (*h*)	Areal storm depth* (mm)	Max1min† (mm/h)	Max Depth‡ (mm)
1	WGEW	06/17/1999 14	3	2.1	150	26.7
2	WGEW	07/06/1999 18	3	10.2	148	28.8
3	WGEW	07/14/1999 10	14	43.9	260	89.0
4	WGEW	07/25/1999 17	3	1.7	232	25.2
5	WGEW	08/02/1999 16	6	10.0	152	28.8
6	WGEW	08/18/1999 14	3	2.1	166	16.2
7	WGEW	08/28/1999 16	5	19.7	230	37.7
8	WGEW	08/31/1999 15	5	16.4	219	47.8
9	WGEW	06/18/2000 16	3	3.1	129	23.7
10	WGEW	06/29/2000 11	3	15.2	182	57.6
11	WGEW	07/16/2000 17	6	7.1	113	29.5
12	WGEW	08/06/2000 18	7	25.3	326	55.8
13	WGEW	08/11/2000 11	4	24.0	391	90.4

* Average of all gauge data available. For the WGEW study area, all the gauges are located within the watershed.
† Maximum 1-min rainfall intensity recorded at a gauge.
‡ Maximum storm depth recorded at a gauge.

Research Service of the US Department of Agriculture (USDA-ARS). Rain data from 74 gauges, which passed quality control, were used for radar calibration and in the evaluation procedure.

The watershed is located 50 to 70 km east-southeast of the US National Weather Service (NWS) Tucson WSR-88D weather radar. Radar data from an 1125-km^2 segment encompassing the watershed were used (see Figure 1b). Because radar beams at the first and second tilts are partially blocked by terrain before they reach the watershed (Morin *et al.*, 2003), only the third tilt data (elevation angle of 2.4°, equivalent to 3-km altitude above ground over the study area), were used for the analysis.

Radar reflectivity data (Z) [mm^6 m^{-3}] are converted to rain intensity data (R) [mm/h] using a power law Z–R relationship $Z = aR^b$. The exponent parameter (b) was set to the value of 1.4 that is used by the NWS for convective rainfall (Fulton *et al.*, 1998), while the multiplicative parameter (a) was adjusted on the basis of comparison of gauge and radar storm depth data. The resulting Z–R relationship, based on analysis of

radar and gauge data for the selected 13 storms over WGEW, was

$$Z = 655R^{1.4} \quad (1)$$

An upper threshold of 100 mm/h was applied to the estimated rain intensity. This is a default threshold rain intensity used by the NWS to reduce unreasonably large estimates caused by hail cores in thunderstorms (Fulton *et al*., 1998).

3. Rainfall modeling

The conceptual rainfall model used in this study to represent spatial structures of rainfall is a deterministic version of the model proposed by Rodriguez-Iturbe *et al*. (1986). Using rain gauge data, the model was found suitable for representing the spatial variability of storm rain depth in the WGEW (Eagleson *et al*., 1987). The model assumes that rain intensity fields are composed of multiple rain cells. Each rain cell is an isotropic circular element with maximum rain intensity at the center and a quadratic exponential decay with distance from the center:

$$R_i(d) = \beta_i e^{-2\alpha_i^2 d^2} \quad (2)$$

where $R_i(d)$ is rain intensity [mm/h] for rain cell i at a distance d [km] from the rain cell center at coordinates (X_i, Y_i), β_i is the rain intensity [mm/h] at the center of rain cell, and, α_i is the decay parameter [km^{-1}] of rain cell i. Equation 2 defines a two-dimensional nonnormalized Gaussian surface, where β_i represents the amplitude and α_i represents the spatial extent.

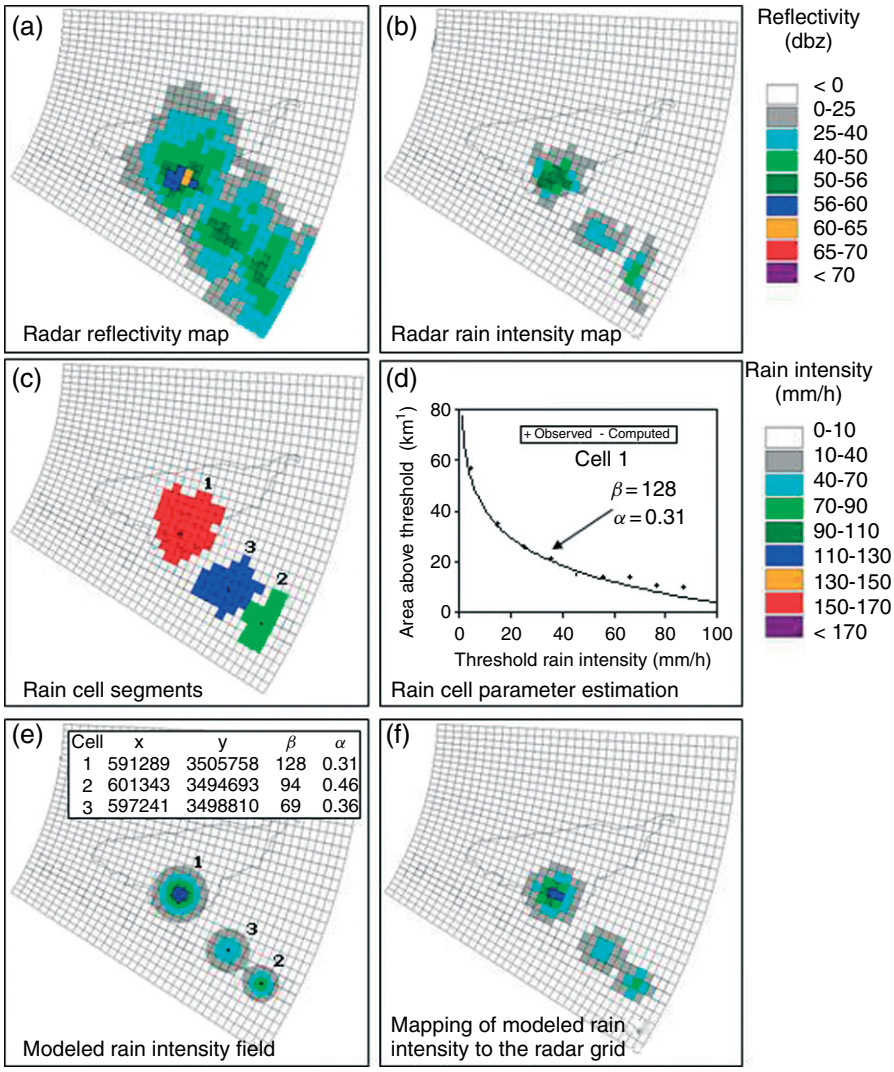

Figure 2. Illustration of model application for radar data from the storm of July 6, 1999 at time 14:45 (LTC). (a) Radar reflectivity map. (b) Radar rain intensity map upon application of the $Z-R$ relationship described in Section 2. (c) Rain cell segments. Black dots show the center of maximum pixels and are considered as the rain cell center locations. (d) Parameter estimation for rain cell 1. Observed area above threshold (A^τ) for threshold values (τ) between 5 and 100 mm/h are indicated (circles). The α parameter is estimated on the basis of these values. The β parameter is estimated from the resultant α and the estimated rain cell integral. The computed curve resulting from the estimated α and β parameters is shown. (e) Model results for the given radar rainfall map. Three rain cells were identified. The four parameters for each rain cell are shown in table (location in UTM coordinates). Figure shows the resulting rain intensity field plotted on 100 × 100-m grid. (f) Mapping of the modeled rain intensity field to the radar-grid pixels for comparison with the observed radar rain intensity map (b)

Parameter α_i is equivalent to the inverse of two times the standard deviation of the Gaussian distribution.

A procedure was developed for estimating model parameters for each radar map (Figure 2). The main computational steps in this procedure are as follows: (1) input radar reflectivity map, (2) convert radar reflectivity to radar rainfall intensity, (3) segmentation, (4) eliminate or merge small and weak segments, (5) determine the rain cell parameters and (6) model output: number of rain cells for each radar map and four model parameters for each cell. These steps are repeated for the series of radar maps of a given storm. The algorithm produces a description of the rain cells (number, location and parameters) as they evolve throughout the storm.

The algorithm was applied to radar data from 13 storms over the WGEW, which included 1438 radar maps. Three hundred seventy seven rain cells were identified in these maps. Summary of their characteristics are presented in Figure 3 and Table II. Figure 3d presents an example of the modeled rain cells over WGEW for four time steps in the 6 July 1999 storm.

The modeled cell center rain intensity parameter (β) varies over a relatively large range (mean = 61.5 mm/h, standard deviation = 42.3 mm/h), while the distribution of the decay parameter (α) shows small variability (mean = 0.39 km^{-1}, standard deviation = 0.08 km^{-1}). Physically, the latter observation indicates that at 2.5 km (2.1–3.2 km) distance from the cell center the rain intensity is reduced to 14% of its intensity at the center. Rapid decline in rain intensity was previously reported in other studies of the Arizona region (Osborn and Renard, 1988). Our estimation

Table II. Summary of modeling results

Storm	Maps with cells	Total number of cells	β, mm/h			α, km^{-1}		
			Aver.	Min.	Max.	Aver.	Min.	Max.
1	19	49	51	11	225	0.37	0.25	0.54
2	29	112	47	13	193	0.38	0.15	0.67
3	86	370	62	11	228	0.41	0.23	0.67
4	13	28	90	20	239	0.46	0.34	0.67
5	29	80	44	11	129	0.40	0.22	0.53
6	17	35	58	14	142	0.44	0.31	0.60
7	30	124	70	14	211	0.39	0.22	0.63
8	39	167	74	9	225	0.36	0.19	0.57
9	12	36	47	16	132	0.38	0.25	0.54
10	28	129	65	14	203	0.41	0.26	0.58
11	31	72	41	10	95	0.41	0.29	0.60
12	21	182	69	13	214	0.37	0.15	0.56
13	23	54	86	12	247	0.39	0.25	0.55

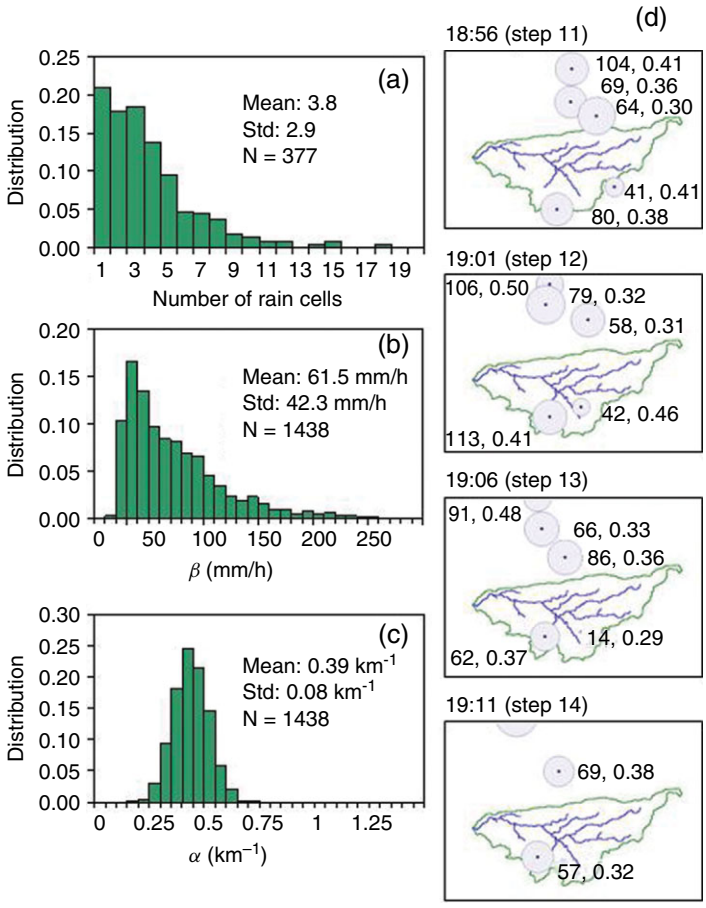

Figure 3. Histograms of computed model parameters for 13 storms over the WGEW study area: (a) number of rain cells, (b) β parameter and (c) α parameter. (d) Modeling results for the storm of July 6, 1999 over the WGEW study area. Rain cells at time steps 11 to 14 (18:56–19:11 LTC). The cell center and the 25-mm/h contour (for cells with $\beta > 25$ mm/h) are plotted. The two numbers near each rain cell are the cell center intensity, β (in mm/h) and the decay parameter, α (in km^{-1}) parameters

of α is supported by Eagleson *et al*. (1987), which reported an estimated mean value of $\alpha = 0.43$ km^{-1} and standard deviation of 0.17 km^{-1} over a set of 426 storms.

4. Evaluation of rainfall model

An important step in this study was to evaluate the modeled radar rainfall using a different (ideally independent) dataset. For this, we used the dense gauge network in the WGEW (an average of one gauge in 2 km^2, Figure 1). Although these data had already been used to remove the overall bias from the radar rainfall estimations (Section 2), they still provided a set of relatively independent observations.

The evaluation process includes comparison of several rainfall sources as follows: radar-modeled rainfall, gauge-modeled rainfall, radar-grid rainfall and gauge-interpolated rainfall.

Several evaluation tests were applied in order to examine the different aspects of the model results. Summary of the main findings in these tests are given below:

1. Radar rainfall modeling was able to identify most (71%) of the gauge-modeled rain cells at a relatively close distance (2 km on average). A moderate fit of radar-modeled and gauge-modeled rain cell parameters was found (correlations of 0.65 and 0.5 for the β and α parameters, respectively).
2. Radar-modeled rain cells are characterized by higher (+27% bias) β parameter values relative to gauge-modeled rainfall. Possible explanations are altitude differences and the effect of evaporation.
3. Gauge-modeled rain cells are in general larger (+52%) than the radar-modeled rain cells and the rain field is characterized by higher spatial correlation. We suspect this to be a result of inadequate spatial sampling by the gauge network. The outcomes are lower α parameter values (−15%) and smoother rain fields.
4. Modeled rainfall (gauge and radar) represents only convective rain pixels in data. This results in underestimation (−32% on average) of areal rainfall as compared to the gauge-interpolated rainfall. Correlation of areal rainfall between radar-modeled and the gauge-interpolated rainfall is relatively good (0.89, 0.75, 0.66 for watershed size, 4×4 km area and 1×1 km area, respectively).

5. Modeled rainfall as input to hydrological model

The above sections presented rainfall modeling in the form of rain cells. In this approach, each rainfall map is translated into a set of rain cells specified by their location, maximum rain intensity and decay factor. Because this modeling process recognizes rainfall spatial patterns that may play an important role in runoff generation, we evaluated the possibility of using the modeled rainfall as input to a hydrological model.

We analyzed the rainfall-runoff event of 11 August 2000, which totaled 25-mm watershed average rainfall depth with a maximum gauge depth of 91 mm and a recorded runoff peak discharge of 154 cm at the watershed outlet.

The hydrological model used is the KINEROS2, a physically based, event oriented, rainfall-runoff model (Woolhiser *et al*., 1990; Smith *et al*., 1995) developed by USDA-ARS scientists for watersheds in semiarid environments. The model represents the watershed as a cascade of overland flow planes and channels, thereby allowing rainfall, infiltration, runoff and erosion parameters to vary spatially. Recently, a GIS-based tool (AGWA) was developed by the USDA-ARS (Miller *et al*., 2002) for delineating watersheds into hillslope-contributing areas (abstracted into overland flow plane model elements) and channels and generating model parameter files, based on topography, soil and land cover information. In this study, we used the KINEROS2 model with default parameters generated by AGWA for the WGEW (delineation of 53 planes — average area 2.8 km^2 and 21 channels).

Two rainfall inputs were analyzed using the hydrological model. The first was the radar-grid rainfall data and the second was the radar-modeled rainfall data. Figure 4a presents the two computed runoff hydrographs at the watershed outlet. It should be emphasized that the radar rainfall estimations were based on the $Z-R$ relationship described in Section 2. If the default NWS $Z-R$ relationship for convective precipitation is used (Fulton *et al*., 1998), the computed runoff peak discharge is more than three times higher.

Comparing the two computed runoff hydrographs in Figure 4a, only minor differences were revealed. This suggests that both inputs contain essentially the same information required for predicting the hydrological response (as represented by the hydrological model). We believe that by using the rain cell analysis representation, a better understanding can be gained of the major factors that generate runoff.

A manual examination and tracking of the modeled rain cells in the 11 August 2000 rainfall-runoff event (Figure 4b, Table III) identified five rain cells (cells A–E) that developed close to or over the watershed. Two of the modeled cells (A and C) were intense (in terms of maximum intensity and volume) and lasted a relatively long time (more than 60 min). The modeled cell A initiated outside and north of the watershed and then moved southward into the watershed. The modeled cell C developed within the watershed and moved west-northwest toward and beyond the watershed outlet. The three other cells (B, D and E) moved generally northward, had shorter duration (15 min) and were less intense.

Comparison of the computed runoff response for each modeled cell separately indicates that only cell C

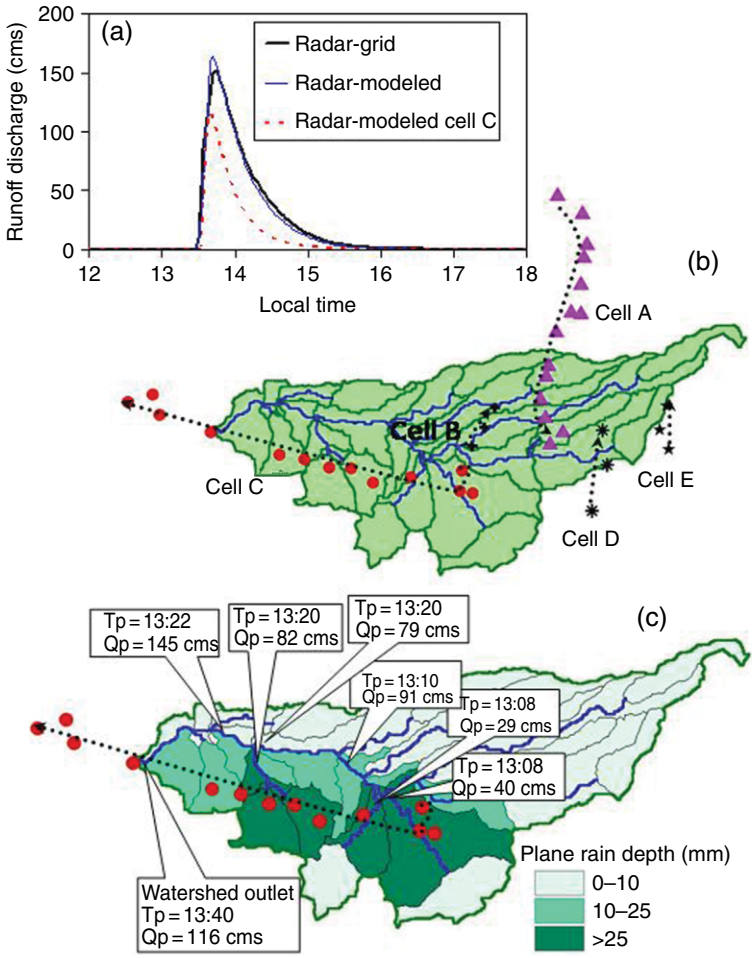

Figure 4. (a) Computed runoff hydrographs at the WGEW outlet using the KINEROS2 rainfall-runoff model for the August 11, 2000 storm with different inputs: radar-grid rainfall (thick solid line), radar-modeled rainfall (thin solid line) and radar-modeled rainfall with only rain cell C (see Figure 4b) active (thin dashed line). (b) Modeled rain cells locations and trajectories over WGEW for the August 11, 2000 storm. Rain cell tracking was done manually. (c) Computed response of model elements in relation to rain cell location and trajectories for the August 11, 2000 storm over the WGEW. Averaged rain depth contributed by the modeled rain cell C to each overland flow plane is shown. For selected points along the channel network, the time of peak discharge (Tp) and peak discharge (Qp) are presented

Table III. Rain cell characteristics in the storm of August 11, 2000

Cell	Start time	Duration, min	Maximum intensity, mm/h	Volume, m^3	Rain over WGEW, mm
A	11:58	70	170	1.54×10^6	5.3
B	12:23	15	138	0.28×10^6	2.3
C	12:41	65	247	2.32×10^6	12.5
D	13:06	15	150	0.27×10^6	1.0
E	13:21	15	92	0.17×10^6	0.0

contributed to the peak discharge at the watershed outlet (Figure 4a, dashed line). This is probably due to its location within the watershed for most of its life cycle. Another important factor is the specific configuration of rain cell C relative to the watershed. Examining the detailed response of each model element (overland flow planes and channels) revealed that the cell passed close to watershed tributaries at three locations, precipitating more than 25 mm of intense rainfall over their associated contributing areas. This generated significant excess rainfall over the associated runoff model elements and high peak flows at the tributaries to the main channel (Figure 4c). The flow toward and along the main channel was such that runoff peaks arriving from the tributaries were close in time to the runoff peak of the main channel, resulting in an intensification of the peak flow. Over the last 7 km of the channel, there was no lateral contribution to the flow from hillslope areas or tributaries, which resulted in reduction of peak flow due to channel transmission losses.

In view of the above description, it is clear that different configurations of rain cells relative to the watershed can yield different runoff responses. Using the rainfall input in the form of modeled rain cell representation enables examination of runoff sensitivity to realistic rain cell characteristics (such as location, direction, velocity, spread and maximum intensity). Figure 5a presents sensitivity of runoff peak discharge to direction of rain cell C obtained by rotating the observed track of the rain cell by a given angle. These results indicate that the observed cell direction enhance

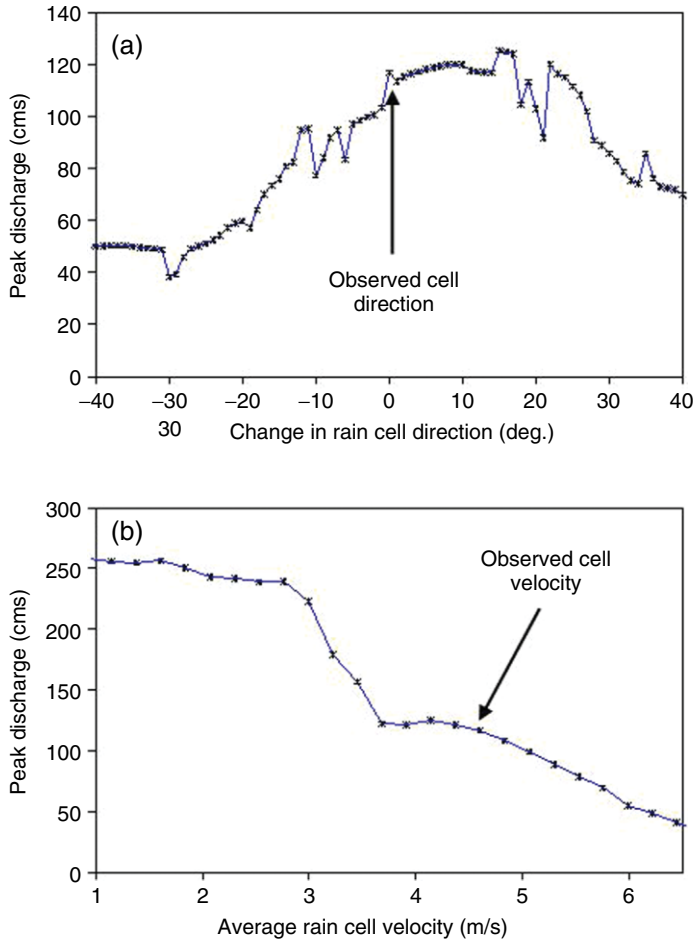

Figure 5. Sensitivity of computed runoff peak discharge at the watershed outlet to (a) direction of rain cell C and (b) velocity of rain cell C

runoff peak discharge for the reasons stated above. According to the model, the peak discharge would be 8% higher if the cell direction were rotated 15^o clockwise from its current direction. In that case, locations of high intensity rainfall are closer to the watershed main channel, resulting there in high discharges. Sensitivity analysis to rain cell velocity (Figure 5b) indicates potential for significant increase in peak discharge for slower rain cell (velocity less than 3 m/s). The increase in peak discharge is resulted from the relatively large rainfall amounts that are rained over the same area, causing large runoff amounts to be generated and to flow toward the outlet.

The analysis shown here is limited to the hydrological response as represented by the hydrological model. The main goal is to demonstrate the potential of using modeled rainfall as input to a hydrological model. Further research needs to be conducted to examine the advantages and disadvantages of this approach from a more general perspective.

6. Summary and conclusions

The article presents the application of a conceptual rainfall model to observed radar data and the input of the modeled rainfall into a distributed hydrological model. We suggest that by using this approach, rainfall structures are explicitly represented in the hydrological model input, which allows a direct linkage between rainfall structures and watershed hydrological response.

Applying the rainfall model to radar data yields rainstorm representation as a set of convective rain cells with a limited set of characteristic variables. The modeled rainfall has a relatively simple structure, but includes all the main spatial features of rainfall patterns: location and magnitude of maximum rainfall intensity, rain–no rain areas (rain cell coverage) and small-scale variability (within rain cells). These features are important characteristics of the rain system and are known to play a significant role in watershed response to rainfall. The rainfall model was applied to radar data of 13 air mass thunderstorms in southeastern Arizona and evaluated using a dense rain gauge network.

We explored the potential use of modeled rainfall as input to a distributed hydrological model. Although the original radar rainfall data produced a similar computed runoff hydrograph as the modeled rainfall, it is the added insights that can be acquired on the spatial watershed response behavior using the latter

that, in our view, makes this approach beneficial. This is because there is an essential difference in the way spatial patterns are represented in modeled radar rainfall data versus the original radar rainfall data. In the modeled rainfall, the spatial patterns are explicitly represented through the model parameters. The modeling process enables the decomposition of complex rainfall patterns into modeled cells with defined parameters and trajectories. In the grid rainfall data, the patterns are implicitly represented, but are not easily quantified into well-defined parameters or functions. For example, location of the rain cell center is a parameter of modeled rainfall. On the other hand, in the grid rainfall field, specific analysis of the data is required in order to obtain the same information.

The explicit representation of rainfall spatial patterns in hydrological model input allows derivation of a more comprehensive link between runoff response and spatial rainfall patterns.

Acknowledgements

This research was partly funded by grants from the International Arid Lands Consortium (IALC, 00R-11) and the Vaadia-BARD Postdoctoral Award No. FI-303-2000 from BARD, The United States — Israel Binational Agricultural Research and Development Fund. The research is based upon work supported in part by SAHRA (Sustainability of semi-Arid Hydrology and Riparian Areas) under the STC Program of the National Science Foundation, Agreement No. EAR-9876800 and by grants from the Hydrologic Laboratory of the National Weather Service, Grants NA87WHO582 and NA07WH0144. We are thankful to the staff members of the Southwest Watershed Research Center, USDA-ARS, for their assistance.

References

Carpenter TM, Georgakakos KP, Sperfslagea JA. 2001. On the parametric and NEXRAD-radar sensitivities of a distributed hydrologic model suitable for operational use. *Journal of Hydrology* **253**: 169–193.

Collinge VK, Kirby C. 1987. *Weather Radar and Flood Forecasting*. Wiley: New York.

Douglas MW, Maddox RA, Howard K, Reyes S. 1993. The Mexican monsoon. *Journal of Climate* **6**(8): 1665–1677.

Eagleson PS, Fennessey NM, Qinliang W, Rodriguez-Iturbe I. 1987. Application of spatial Poisson models to air mass thunderstorm rainfall. *Journal of Geophysics Research* **92**(D8): 9661–9678.

Fulton RA, Breidenbach JP, Seo DJ, Miller DA. 1998. The WSR-88D rainfall algorithm. *Weather and Forecasting* **13**: 377–395.

Goodrich DC, Lane LJ, Shillito RA, Miller SN, Syed KH, Woolhiser DA. 1997. Linearity of basin response as a function of scale in a semi-arid watershed. *Water Resources Research* **33**(12): 2951–2965.

Ichikawa Y, Hori T, Shiiba M, Tachikawa Y, Takara K. 2002. Investigation on the scale of rainfall spatial variability to be considered in runoff simulation. *Journal of Hydroscience and Hydraulic Engineering* **20**(2): 207–216.

Julien PY, Saghafian B, Ogden FL. 1995. Raster-based hydrologic modeling of spatially-varied surface runoff. *Water Resources Bull* **31**(3): 523–536.

Krajewski WF, Smith JA. 2002. Radar hydrology: rainfall estimation. *Advance Water Resources* **25**: 1387–1394.

Michaud JD, Sorooshian S. 1994. Effect of rainfall-sampling errors on simulations of desert flash floods. *Water Resources Research* **30**(10): 2765–2775.

Miller SN, Semmens DJ, Miller RC, Hernandez M, Goodrich DC, Miller WP, Kepner WG, Ebert D. 2002. GIS-based hydrologic modeling: the automated geospatial watershed assessment tool. *Proceedings. of the Second Federal Interagency Hydrologic Modeling Conference*, Las Vegas NV, July 28–August 1.

Morin E, Krajewski WF, Goodrich DC, Gao X, Sorooshian S. 2003. Estimating rainfall intensities from weather radar data: The scale dependency problem. *Journal of Hydrometeorology* **4**(5): 782–797.

Osborn HB, Renard KG. 1988. Rainfall intensities for SE Arizona. *Journal of Irrigation and Drainage Engineering* **114**: 195–199.

Rodriguez-Iturbe I, Wang Q, Jacobs BL, Eagleson PS. 1986. Spatial modeling of total storm rainfall. *Proceedings of the Royal Society of London* **A403**: 27–50.

Smith RE, Goodrich DC, Woolhiser DA, Unkrich CL. 1995 KINEROS — a kinematic runoff and erosion model.. In *Computer Models of Watershed Hydrology*, Singh VP (ed.) Water Resources Publications: Highlands Ranch, Colorado; 697–732.

Wallace CE, Maddox RA, Howard KW. 1999. Summertime convective storm environments in central Arizona: local observations. *Weather and Forecasting* **14**(6): 994–1006.

Winchell M, Gupta HV, Sorooshian S. 1998. On the simulation of infiltration- and saturation-excess runoff using radar-based rainfall estimates: effects of algorithm uncertainty and pixel aggregation. *Water Resources Research* **34**(10): 2655–2670.

Woolhiser DA, Smith RE, Goodrich DC. 1990. KINEROS, A kinematic runoff and erosion model: Documentation and user manual. U.S. Dept. of Agriculture, Agricultural Research Service, ARS-77.

